Shear Resistance of Concrete Beams under Decade of Sustained Loading

Sarkhosh, Reza; Walraven, Joost

DOI
10.14359/51743303

Publication date
2025

Document Version
Final published version

Published in
ACI Structural Journal

ACI STRUCTURAL JOURNAL TECHNICAL PAPER

Title No. 122-S25

Shear Resistance of Concrete Beams under Decade of Sustained Loading

by Reza Sarkhosh and Joost Walraven

Subjected to either tensile or compressive loads, concrete is susceptible to the effect of sustained loading. To address this, common practice in building guidelines typically involves applying a sustained loading factor ranging from 0.6 to 0.85. Given that the shear capacity of structural members without shear reinforcement is linked to the concrete strength, one might question whether there is a comparable sustained loading impact on shear. To address this inquiry, a total of 18 reinforced concrete beams without shear reinforcement were subjected to prolonged sustained loading, with a load intensity factor (ratio of applied sustained shear load to short-term shear resistance) ranging from 0.88 to 0.98. Several beams endured the sustained loading test for an extended period, close to a decade, before the test was terminated. Interestingly, in contrast to concrete subjected to direct compression or tension, it was observed that sustained loading did not affect the shear capacity. Some early results of this experimental study, where concrete beams were subjected to up to 4 years of sustained loading, have been previously published by Sarkhosh and Sarkhosh et al. This paper concludes the results of the testing campaign of up to a decade of sustained loading, with additional results and findings.

Keywords: beam; long-term loading; reinforced concrete; shear; sustained.

INTRODUCTION

In recent years, significant emphasis has been placed on assessing the bearing resistance of existing bridges. The primary cause for this concern stems from the increasing traffic loads and potentially outdated reinforcement details, which cast doubts on the structural integrity. As part of a comprehensive national evaluation of numerous bridges in the Netherlands, a meticulous examination was conducted, focusing on the bearing resistance of various structural types, including a substantial quantity of solid slabs lacking shear reinforcement.

One advantage of aging in concrete structures lies in the substantial increase in actual strength compared to the design strength established many years ago, typically at 28 days of age. This enhanced strength is a result of the ongoing process of cement hydration, which extends well beyond the initial 28-day period. Older cements, in particular, featured coarser cement particles. During the early stages of hydration, a hardened cement skin forms on the outer surface of these particles, which hinders the penetration of water to the unhydrated core within. To achieve full hardening of the inner portion of the cement particles, water must first permeate through this hardened skin. Over time, this skin thickens, leading to a slower but prolonged hydration process, continuing long after the initial 28 days. Consequently, the ultimate concrete strength far exceeds the values upon which the original 28-day design strength was based.

While the original design calculations might have been based on a concrete strength class such as C20/25, contemporary tests on drilled cylinders often reveal strength values ranging from 50 to 100 N/mm^2 (7252 to 14,504 psi). When assessing whether concrete slab bridges without shear reinforcement meet current structural safety standards, this heightened concrete strength can be seen as a significant advantage. It is worth noting that, as per all governing codes, shear resistance is intrinsically linked to concrete strength. For instance, the Eurocode EN 1992-1-1:2023[1] includes an expression that demonstrates this relationship

$$V_{Rd,c} = C_{Rd,c}(100\rho_l f_{ck})^{1/3} b_w d \geq v_{min} b_w d \quad \text{[N, mm, N/mm}^2\text{]} \tag{1a}$$

$$(V_{Rd,c} = 130 C_{Rd,c}(100\rho_l f_{ck})^{1/3} b_w d \geq v_{min} b_w d \text{ [lb, psi, in.]})$$

$$\text{with } v_{min} = 0.035 k^{3/2} \cdot f_{ck}^{1/2} \text{ [N, mm, N/mm}^2\text{]} \tag{1b}$$

$$(v_{min} = 0.42 k^{3/2} \cdot f_{ck}^{1/2} \text{ [lb, psi, in.]})$$

where $C_{Rd,c}$ is the design coefficient and recommended to be $0.18/\gamma_c$; k is the size factor, where $k = 1 + (200/d)^{1/2} \leq 2.0$ with d in mm and $k = 1 + (7.9/d)^{1/2} \leq 2.0$ with d in in.; ρ_l is the longitudinal reinforcement ratio, where $\rho_l = A_{sl}/b_w d$; A_{sl} is the cross-sectional area of the tensile reinforcement; b_w is the smallest web width in mm or in., respectively; d is the effective depth of the cross section in mm or in., respectively; γ_c is the material safety factor, which can be taken as 1.0 for calculating the mean value of shear resistance; and f_{ck} is the characteristic compressive strength based on cylindrical samples—in ACI, this value is given as f_c'.

In various codes and standards, such as EN 1992-1-1:2023 or ACI 318-19,[2] the characteristic compressive strength of concrete, f_{ck}, is linked to concrete tensile strength, f_{ct}, generally expressed as

ACI Structural Journal, V. 122, No. 2, March 2025.
MS No. S-2023-308.R1, doi: 10.14359/51743303, received July 29, 2024, and reviewed under Institute publication policies.

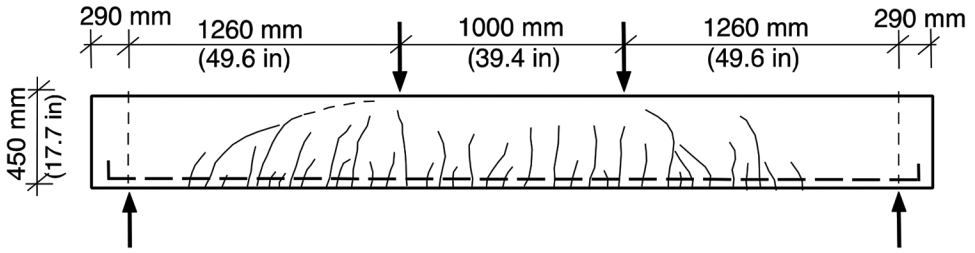

Fig. 1—Beam without shear reinforcement at onset of shear failure.

$$f_{ct} = C \cdot f_{cc}^{n} \tag{2}$$

According to EN 1992-1-1:2023,[1] using the general expression (Eq. (2)), the following relationship is established between the characteristic concrete tensile strength, f_{ctk}, and the characteristic concrete compressive strength, f_{ck}

$$f_{ctk} = 0.21 f_{ck}^{2/3} \text{ [MPa]} \text{ (for } f_{ck} < 50 \text{ MPa)}$$
$$(f_{ctk} = 1.1 f_{ck}^{2/3} \text{ [psi]}) \text{ (for } f_{ctk} \leq 7140 \text{ psi)} \tag{3}$$

ACI 318-19[2] recommends using the modulus of rupture, f_r, as the failure criterion, which is the maximum tensile bending stress in a plain concrete, equal to $0.62\sqrt{f_c'}$.

The rationale behind using the concrete compressive strength instead of the tensile strength in equations for shear resistance, such as Eq. (1a), is due to the fact that the compressive strength is typically measured in standard quality control tests. However, it is important to recognize that the shear resistance of structural members lacking shear reinforcement is fundamentally more influenced by the concrete tensile strength than the concrete compressive strength. This becomes apparent when observing the behavior of a concrete beam under shear loading conditions. Failure in such cases often results from the unstable propagation of an inclined crack, ultimately leading to an explosive type of concrete member failure. Figure 1 illustrates the crack pattern in a shear-reinforcement-free beam with a longitudinal reinforcement ratio $\rho_l = 0.75\%$ and a characteristic compressive strength of 27 MPa (3900 psi) when the load reached 97% of its shear resistance. Shortly thereafter, one of the inclined cracks began to develop progressively (indicated by the dashed line), ultimately leading to structural failure, as described by Walraven.[3]

When assessing the shear resistance of an existing reinforced concrete structure, a crucial consideration arises regarding the possible influence of sustained loading. Existing research has established that sustained loading can lead to a decrease in the tensile strength of concrete. Consequently, in EN 1992-1-1:2023, the design tensile strength is formulated as such to account for this effect.

$$f_{ctd} = \alpha_{ct} \cdot f_{ctk} / \gamma_c \tag{4}$$

where f_{ctk} is the characteristic concrete tensile strength; γ_c is the material safety factor; and α_{ct} is the sustained loading factor, which may be chosen by European countries as a nationally defined parameter in the range $0.8 \leq \alpha_{ct} \leq 1.0$. In the *fib* Model Code,[4] the lower value of the sustained loading factor for the concrete tensile strength, α_{ct}, is as low as 0.6 for normal-strength concrete and 0.75 for high-strength concrete.

Many European countries have, nevertheless, adopted a sustained loading factor $\alpha_{ct} = 1.0$, arguing that the effect of sustained loading is compensated by the increase in concrete strength after 28 days. However, if the strength of the concrete is determined through drilled cylinders, taken from the structure decades after casting, the compensating effect of an increase in the concrete strength obtained by virtue of ongoing hydration does not apply anymore. It was therefore regarded as a matter of utmost importance to find out whether the sustained loading effect not only applies to members subjected to axial compression or tension but also to the shear resistance of concrete members without shear reinforcement. According to the worst scenario, the advantage of using the higher concrete strength to determine the shear resistance might be fully lost if a sustained loading factor also has to be applied for the shear resistance. Consequently, hundreds of bridges would have to be strengthened. It was therefore decided to carry out this experimental investigation to answer this important question.

RESEARCH SIGNIFICANCE

In 2020, research by Tasevski et al.[5] emphasized that more experimental data on long-term shear tests are needed to study the impact of high levels of sustained load and its potential negative effect on shear strength. Over the course of the last decade, an extensive experimental investigation was undertaken at Delft University of Technology to determine the impact of sustained loading on crack propagation in structural elements under pure bending. Furthermore, beams lacking shear reinforcement underwent tests with increasing loads applied in short duration to establish reference values for shear resistance. These tests also provided insights into failure mechanisms, enabling comparisons with subsequent sustained loading tests. The sustained loading tests maintained a load intensity (ratio of applied sustained shear load to short-term shear resistance) between 0.88 and 0.98, offering valuable insights into structural behavior under extreme loading conditions.

EXPERIMENTAL ANALYSIS OF CRACK PROPAGATION IN BENDING UNDER SUSTAINED LOADING

The failure of a beam under shear typically results from the gradual propagation of one of the inclined shear cracks. In the instance depicted in Fig. 1, the load application was relatively rapid, with the time span from the initiation of

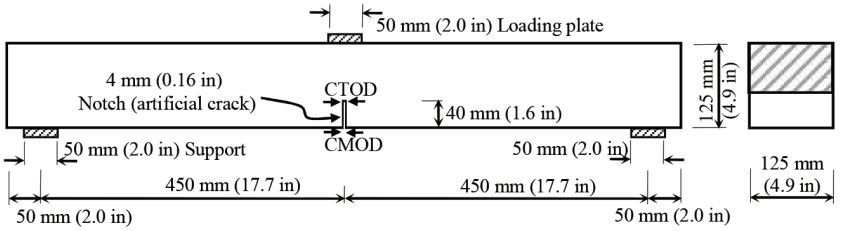

Fig. 2—Test beam with notch for studying crack propagation under sustained loading.

loading to shear failure occurring within approximately 2 to 3 hours.

The initial question to be addressed pertained to whether the sustained loading factor in tension, typically ranging from 0.6 to 0.85, is also applicable to the phenomenon of crack propagation in bending.

Unreinforced specimens

The initial phase of testing involved unreinforced concrete beams with dimensions outlined in Fig. 2. The concrete composition consisted of 330 kg/m^3 (20.6 lb/ft^3) of CEM III/B 42.5 cement, 803 kg/m^3 (50.13 lb/ft^3) of 0.125 to 4 mm sand, 1065 kg/m^3 (66.49 lb/ft^3) of 4 to 16 mm (0.16 to 0.63 in.) gravel, and 165 kg/m^3 (8.43 lb/ft^3) of water, using glacial river aggregate. Notably, a notch with a depth of 40 mm (1.57 in.) was introduced on the tensile side of each beam.

During the loading process, measurements were taken both at the bottom face of the beam (crack mouth opening displacement [CMOD]) and the top of the notch (crack tip opening displacement [CTOD]). These specimens closely resembled those used in previous work by Zhou and Hillerborg.[6] To establish reference values for the sustained loading tests, a set of beams initially underwent short-term deformation controlled by deflection at midspan. This approach allowed the observation of the failure process until the specimen could no longer bear any load.

Unreinforced specimen under sustained loading

Following the short-term loading phase, another group of beams was subjected to sustained loading. In this procedure, the load was applied to a specific level relative to the ultimate short-term load and then maintained at that level until failure occurred. The loading level was characterized by the parameter $\lambda = P_{long}/P_{short}$. The results of these tests are presented in Fig. 3.

At the highest sustained loading intensity of λ = 0.88, failure transpired after 1000 seconds, approximately 17 minutes. For load intensities beyond 0.88, no specimen could withstand the sustained loading for a detectable period, resulting in immediate failure. Hence, no data were collected for those cases. Conversely, at the lowest sustained loading level of λ = 0.7, failure emerged after an extended 73-day period. According to Sarkhosh,[7] under long-term loading conditions, the evolution of crack opening displacement can be explained by a time-dependent concrete strain modeled using the equivalent modulus of elasticity. If the concrete tensile stain at time t exceeds the critical strain (which is also explained as a time-dependent phenomenon), the concrete

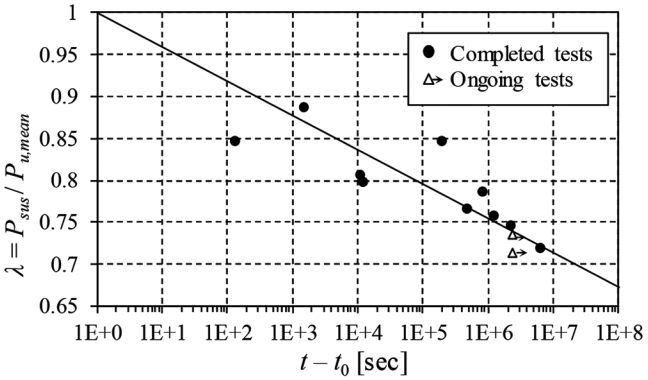

Fig. 3—Results of sustained loading tests in bending on unreinforced concrete beams with notch.

specimen fails. This failure was only observed when the load intensity, λ, was higher than 0.7.

In conclusion, the first series of unreinforced specimens under long-term sustained loading proved that the response of plain concrete to sustained tensile loading is subject to the applied load intensity; therefore, a strength reduction factor, as suggested by some codes, should be applicable to unreinforced concrete.

EXPERIMENTAL ANALYSIS OF SHEAR RESISTANCE OF BEAMS WITHOUT SHEAR REINFORCEMENT UNDER SUSTAINED LOADING

The subsequent experiments sought to ascertain whether the observations related to the time-dependent concrete tensile strain at high load intensities, as previously discussed, were also applicable to shear cracks. In essence, this research aimed to explore the response of shear cracks under prolonged sustained loading conditions. To explore this, a number of shear tests were conducted on beams of several concrete classes lacking shear reinforcement. The beams' geometry and loading configuration can be observed in Fig. 4, and specific details of the cross section and concrete strength are provided in Table 1.

Reinforced specimens without stirrups

A total of 42 full-scale reinforced concrete beams were cast in seven separate batches. The longitudinal reinforcement was intentionally overdesigned to prevent flexural failure before shear failure could occur. For the beams in batches 1 to 5, the same concrete mixture was employed as described previously, with an average cube (150 mm^2 [0.23 in.^{2}]) strength of 42 MPa (~6000 psi), equivalent to a cylinder (D = 100 mm [3.94 in.], h = 300 mm [11.81 in.]) strength of roughly 33.6 MPa (4800 psi). In contrast, batches 6 and 7

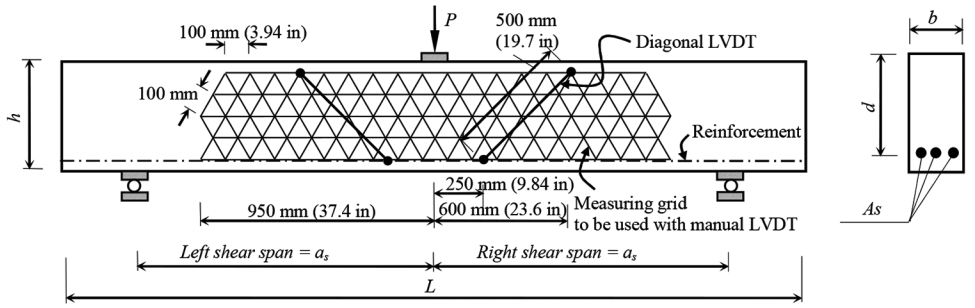

Fig. 4—Reinforced concrete beam specimen subjected to three-point bending.

Table 1—Details of reinforced concrete beams

Batch No.	$f_{c,cube,\ 28days}$*, MPa	h, mm	b, mm	d, mm	L, mm	a_s, mm	a_s/d	A_s, mm^2	ρ, %
1	38.2	450	200	410	3000	1200	2.93	942	1.15
2	34.6	450	200	410	3000	1200	2.93	942	1.15
3	48.4	450	200	410	3000	1200	2.93	942	1.15
4	45.2	450	200	410	3000	1200	2.93	942	1.15
5	44.1	450	200	410	3000	1200	2.93	942	1.15
6	81.2	450	200	407	3000	1200	2.95	1472	1.81
7	80.7	450	200	407	3000	1200	2.95	1472	1.81

*In this research, only cube tests were conducted. For conversion to cylinder strength values or characteristic value, Eurocode 2 recommends $f_{ck} = f_{c,cube} - 8$ (MPa). *fib* Model Code 2020 and other codes[8] recommend a factor of 0.7875 to 0.8$f_{c,cube}$.

Note: 1 MPa = 145 psi; 1 mm = 0.034 in.; 1 mm^2 = 0.00155 in.^{2}.

involved beams constructed using higher-strength concrete, boasting an average cube compressive strength of 81 MPa (11,570 psi), which corresponds to a cylinder strength of approximately 64.8 MPa (9257 psi). In these batches, the same type of gravel was used, featuring a maximum particle diameter of 16 mm (0.63 in.).

Shear resistance

In each of the seven batches, half of the specimens underwent short-term shear loading, leading to shear failure. The load was gradually applied using a manually operated hydraulic system, and the time from zero load to failure was less than 5 minutes. These short-term shear tests were conducted with the purpose of establishing reference values for shear resistance. These reference values served as the foundation for the subsequent sustained loading tests. More comprehensive data on the outcomes of the short-term shear tests for batches 1 to 7 can be found in Table 2.

The coefficient of variation (COV) for any of the subseries of three tests varied between 2.71 and 6.08%, which is relatively small. This was favorable because this means high levels of sustained loading can be installed without a large probability of immediate failure.

Long-term sustained loading

Altogether, 14 beams were subjected to sustained loading. The intensity of sustained loading varied from 88 to 98% of the mean short-term shear resistance. The details of the sustained loading tests are given in Table 3. Moreover, the development of the crack pattern in the beams was monitored. This refers to the crack length and crack width, as well as the change in the distance between the reference points of the measuring grid shown in Fig. 4. On two occasions, shear failure of the beams occurred within 2 days of sustained loading, where no substantial increase in concrete strength due to cement hydration can be assumed; beam S4B6 (Table 3) failed after 2.5 hours of loading, with a sustained loading intensity $\lambda = V_{sus}/V_{u,\ mean\ short}$ of 0.98. Also, beam S7B6 failed in shear after 44 hours with a load intensity of $\lambda = 0.91$. The remaining 12 tests allowed studying the behavior of the beams under sustained loading, focusing on crack propagation, crack width development, and the appearance of new cracks (Fig. 5) during longer periods, even up to 10 years (which coincided with the end of the experimental program). Of course, during this time, for reasons of maintenance of the testing facility, three beams (S3B5, S4B4, and S4B5) had to be unloaded temporarily and reloaded. This can be considered a cyclic loading that could affect the beams' shear capacity; however, no subsequent failure was observed. Although it is difficult to estimate the extent of strength degradation due to unloading and reloading, five cycles of loading and reloading were applied to beam S2B4 at the end of its sustained loading period before testing its ultimate shear resistance. Surprisingly, the beam not only withstood the load cycles but also exhibited an ultimate shear resistance beyond the estimated (calculated) capacity. As explained in this study, the tested capacity of all the beams exceeded the calculated shear capacity.

The goal was to maintain a constant load intensity, λ, throughout the entire sustained loading period on each beam. However, as the concrete strength increased over time, the shear resistance of the beams also increased, leading to a decrease in the real-time load intensity, λ, compared to the initial value defined at t_0. To minimize this effect as much as

Table 2—Shear resistance under short-term monotonic tests

Batch No.	Specimen	Age at t_0, days	Loading time*, seconds	P_u, kN	V_u, kN	$V_{u,mean}$, kN	COV, %	$LCL_{5\%}$†, kN
1	S1B1	28	224	192.03	97.31	93.66	4.53	86.68
	S1B2	28	92	176.14	89.37			
	S1B3	28	194	195.04	98.82			
	S1B4	28	258	174.15	88.37			
	S1B5	32	176	188.03	95.31			
	S1B6	32	162	182.95	92.77			
2	S2B1	70	201	181.82	92.21	95.75	3.07	90.70
	S2B2	71	444	192.76	97.68			
	S2B3	71	191	192.14	97.37			
3	S3B1	83	773	202.69	102.64	102.57	2.71	97.99
	S3B2	83	1697	208.00	105.30			
	S3B3	83	393	204.59	103.59			
	S3B4	87	630	194.88	98.74			
4	S4B1	65	683	187.45	95.02	98.63	4.80	90.84
	S4B2	65	199	191.17	96.88			
	S4B3	65	346	205.39	103.99			
5	S5B1	505	309	199.59	101.09	102.04	3.04	96.93
	S5B2	505	354	199.60	101.10			
	S5B3	505	404	210.50	106.55			
	S5B5	512	558	196.25	99.42			
6	S6B1	89	212	250.33	126.46	123.49	5.13	113.06
	S6B2	89	239	256.80	129.70			
	S6B3	89	194	243.10	122.85			
	S6B5	113	966	227.32	114.96			
7	S7B1	210	495	243.81	123.20	114.78	6.08	103.30
	S7B2	210	256	213.20	107.90			
	S7B3	210	325	232.69	117.64			
	S7B4	219	413	218.14	110.37			

*Time between $P = 0$ and P_u.

†Lower confidence limit $LCL_{5\%}$ = mean – 1.645 SD.

Note: 1 kN = 224.81 lb.

possible, the start of sustained loading was delayed until the concrete had aged for at least 71 days. In batches 5 to 7, the concrete was even older, with the age at the start of sustained loading ranging from 113 to 696 days. The age of the specimen and the sustained loading duration are indicated in the fourth and the last column of Table 3.

For some of the beams—for example, S3B5—subjected to sustained loading for extended periods, the load level was adjusted to account for the expected increase in shear capacity, thereby maintaining a constant load level, λ. This adjustment was made to the beams where an increase in shear capacity of more than 2% was expected. The additional load was applied in the same manner as the original load application using a manually operated hydraulic system.

Observations during sustained loading

Development of midspan deflection and diagonal deformation—Figure 6 provides three examples of beam deformation under sustained loading at loading intensities of λ = 0.97 (S3B5), λ = 0.92 (S6B4), and λ = 0.93 (S7B5). Measurements were taken at the midspan using a vertical linear variable differential transformer (LVDT), and for diagonal deformations, two diagonal LVDTs were employed, as can be seen in Fig. 4 and 5.

(a) Beam S3B5: This beam had a cube strength of 48.5 N/mm^2 (7034 psi) (cylinder strength of approximately 39 N/mm^2 [5656 psi]). Sustained loading at an intensity of λ = 0.97 began at a concrete age of 87 days. After 1344 days of sustained loading, the midspan deflection increased from 3.92 to 6.06 mm (0.154 to 0.24 in.). Notably, the beam experienced a 60-day unloading in between due

Table 3—Beams tested under sustained loading

Batch No.	$V_{u,mean}$, kN	Specimen	Age at t_0, days	P_{sus}, kN	$V_{sus} = (P_{sus}/2) + (m_b g/4)$, kN	$\lambda = V_{sus}/V_u$	Description
2	95.75	S2B4	72	165.1	83.85	0.88	Stopped after 84 days
		S2B5	72	165.1	83.85	0.88	Stopped after 84 days
		S2B6	72	165.1	83.85	0.88	Stopped after 84 days
3	102.57	S3B5	87	196.0	99.30	0.97	Stopped after 1344 days
		S3B6	87	196.0	99.30	0.97	Stopped after 127 days
4	98.63	S4B4	71	185.0	93.80	0.95	Stopped after 274 days
		S4B5	71	185.0	93.80	0.95	Stopped after 274 days
		S4B6	71	190.5	96.55	0.98	Failed after 2.5 hours
5	102.04	S5B4	512	185.0	93.80	0.92	Stopped after 784 days
		S5B6	696	173.0	87.80	0.86	Stopped after 600 days
6	123.49	S6B4	113	224.0	113.30	0.92	Stopped after 3300 days
		S6B6	113	224.0	113.30	0.92	Stopped after 1113 days
7	114.78	S7B5	219	210.0	106.30	0.93	Stopped after 3150 days
		S7B6	219	205.5	104.05	0.91	Failed after 44 hours

Note: 1 kN = 224.81 lb.

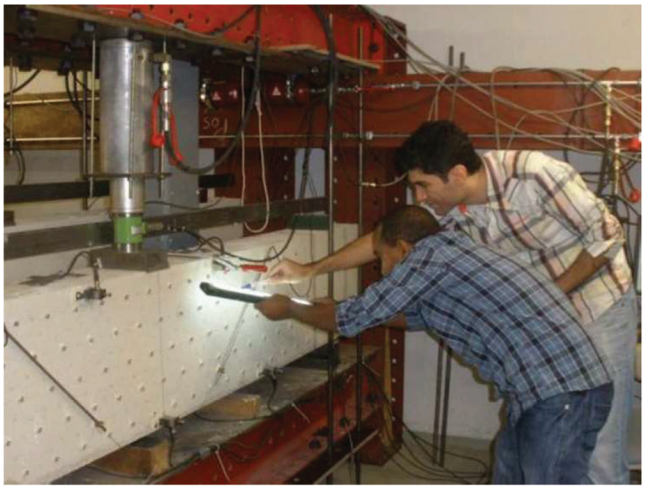

Fig. 5—Measuring distance between reference points.

to climate-controlled room maintenance but was reloaded to the same intensity without a reduction in capacity.

(b) Beam S6B4: This beam had a concrete cube strength of 81.2 N/mm^2 (11777 psi) (cylinder strength of approximately 65 N/mm^2 [9430 psi]). Subjected to 3300 days of sustained loading at an intensity of $\lambda = 0.92$, the midspan deflection increased from 2.95 mm (0.116 in.) at t_0 to 4.46 mm (0.176 in.) at the end of the 3300-day loading. The diagonal deformations were symmetric on both the right and left spans.

(c) Beam S7B5: This beam had a concrete cube strength of 80.7 N/mm^2 (11705 psi) (cylinder strength of approximately 64.6 N/mm^2 [9370 psi]). Subjected to 3150 days of sustained loading at an intensity of $\lambda = 0.93$, the midspan deflection increased from 2.90 mm (0.114 in.) at t_0 to 3.97 mm (0.156 in.) at the end of the 3150-day loading. The diagonal deformations were asymmetric on the right and left spans, with one increasing over time and the other decreasing.

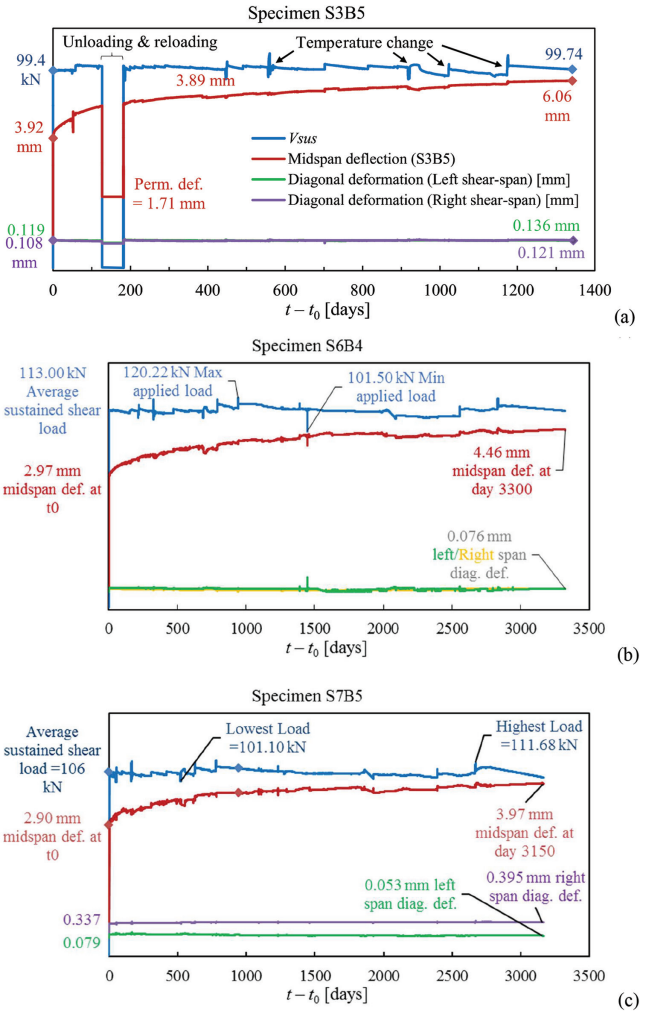

Fig. 6—Deflection and diagonal deformation of: (a) beam S3B5 in 1344 days ($\lambda = 0.97$); (b) beam S6B4 in 3300 days ($\lambda = 0.92$); and (c) beam S7B5 in 3150 days ($\lambda = 0.93$).

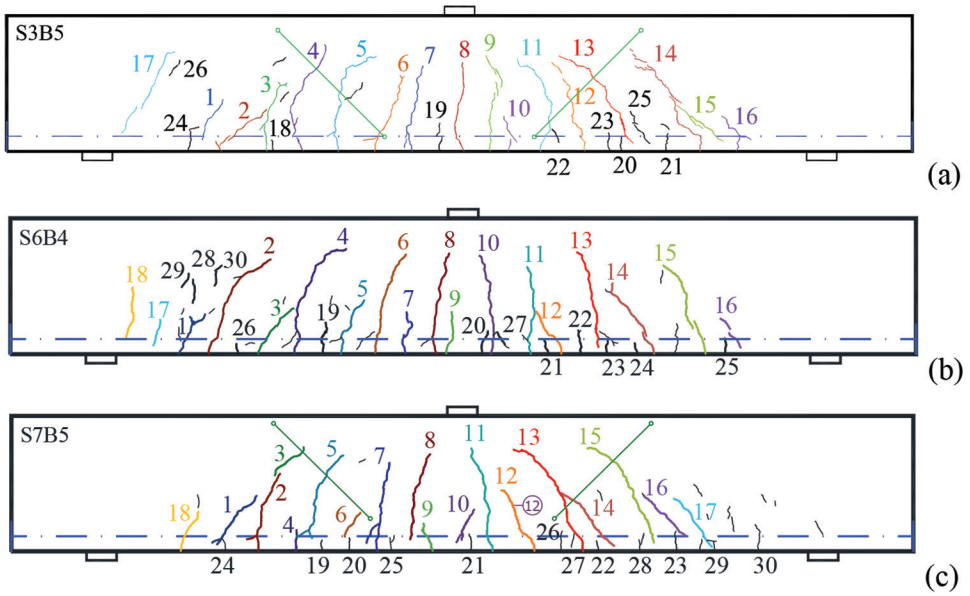

Fig. 7—Crack pattern of: (a) beam S3B5 (λ = 0.97) after 1344 days of sustained loading; (b) beam S6B4 (λ = 0.92) after 1113 days of sustained loading; and (c) beam S7B5 (λ = 0.93) after 3150 days of sustained loading.

Development of crack pattern in time—Throughout the sustained loading tests, the surface crack pattern was closely observed and monitored (Fig. 5). Each crack was assigned a unique identifying number. Monitoring of these cracks commenced immediately after loading ($t = t_0$). The most significant development in the crack pattern occurred during the initial loading phase. Certain shrinkage cracks had already been marked before the onset of sustained loading. However, even at a later age, some cracks at the surface of the beam were likely attributed to short shrinkage cracks. Figures 7(a) to (c) display the surface cracks of the same beams (S3B5, S6B4, and S7B5) that were discussed earlier.

Development of crack length in time—The surface crack pattern of the beams under sustained loading is presented in Fig. 7(a) to (c). The actual image of these beams under sustained loading can be found in Fig. 8. Most of these surface cracks became apparent immediately after the application of the load at t_0, while some continued to propagate over time, and others remained dormant. Additionally, there were instances of cracks appearing at the surface of the beam during sustained loading. All these cracks were assigned unique numbers in Fig. 7(a) to (c), and their length was documented and measured over time.

The results of crack length development are showcased in Fig. 9(a) to (c) for the same beams (S3B5, S6B4, and S7B5) discussed earlier. Surface cracks were categorized into two groups: major cracks and minor cracks. Minor cracks were characterized as short-length cracks (less than 100 mm [3.94 in.]), and it was inferred that these short-length cracks have no direct influence on shear (or flexural) failure. However, they are of sufficient size to potentially impact the stress distribution in the beam. Conversely, major cracks, defined as longer than 100 mm (3.94 in.), are expected to play a role in the beam's failure process.

The graphs of Fig. 9(a) to (c) clearly illustrate that some of the surface cracks propagate over time, while others remain static. The development of crack length is not exclusively limited to major cracks; at times, minor cracks exhibit significant growth, even as major cracks show no progression.

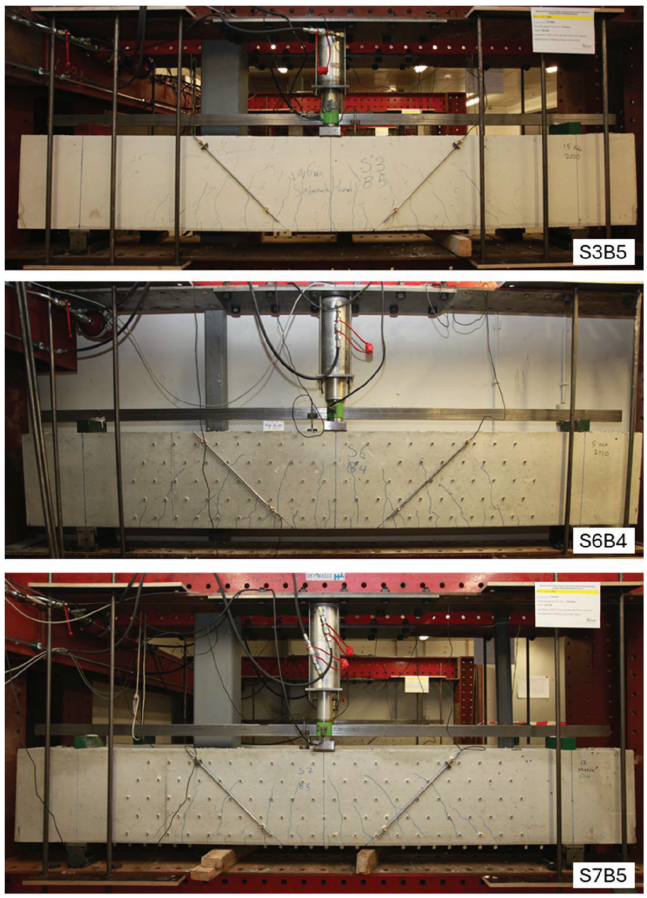

Fig. 8—Beams S3B5, S6B4, and S7B5 under sustained loading.

To mitigate the impact of increasing concrete strength due to cement hydration during long-term loading, the beams were loaded at an age of at least 71 days. Nonetheless, a substantial number of new cracks emerged on the beam's

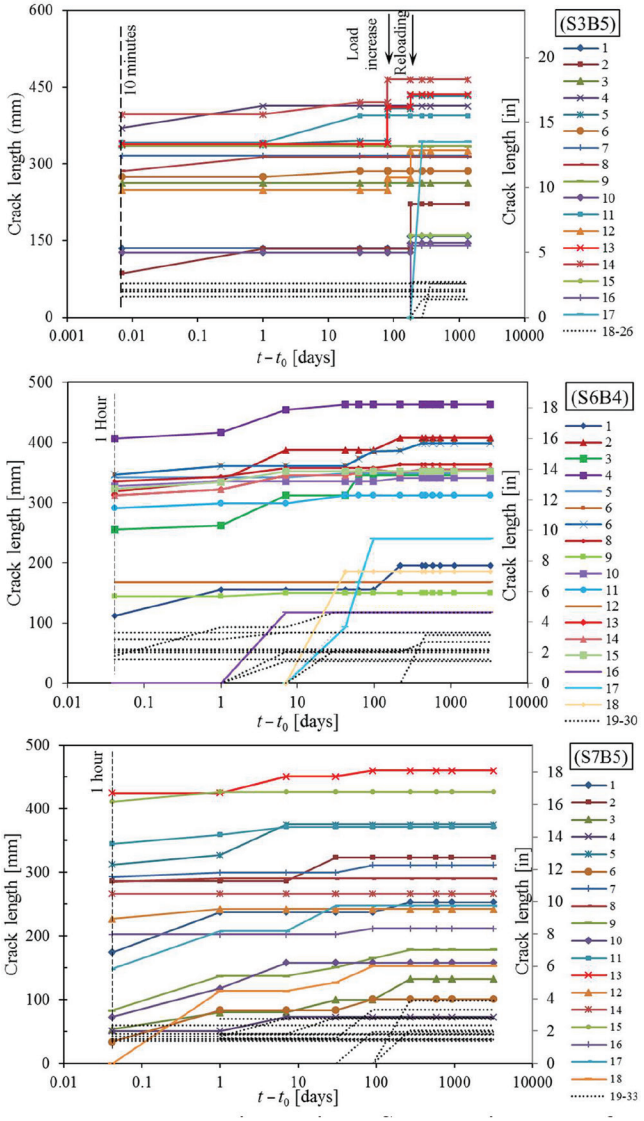

Fig. 9—Crack length development in: (a) Specimen S3B5 during 1344 days of sustained loading (λ = 0.97); (b) specimen S6B4 during 3300 days of sustained loading (λ = 0.92); and (c) Specimen S7B5 during 3150 days of sustained loading (λ = 0.93).

surface during sustained loading, most likely attributed to shrinkage cracks. To provide a more thorough understanding of these new cracks, two specimens (S5B4 and S5B6) were loaded at notably higher concrete ages of 512 days and 696 days. A comparison between the results of crack monitoring in fresh concrete and aged concrete (S5B4 and S5B6) revealed that the majority of new surface cracks that developed during the long-term tests were indeed shrinkage cracks, as the number of new surface cracks during sustained loading was significantly lower in the aged concrete beams.

One important observation made during sustained loading was that the cracks ceased to propagate after 6 months ($t - t_0 > 180$ days) under consistent conditions of temperature, humidity, and external load.

Development of crack width in time—A crack width typically reaches its maximum value at the mouth of the crack and gradually diminishes along the crack length until it

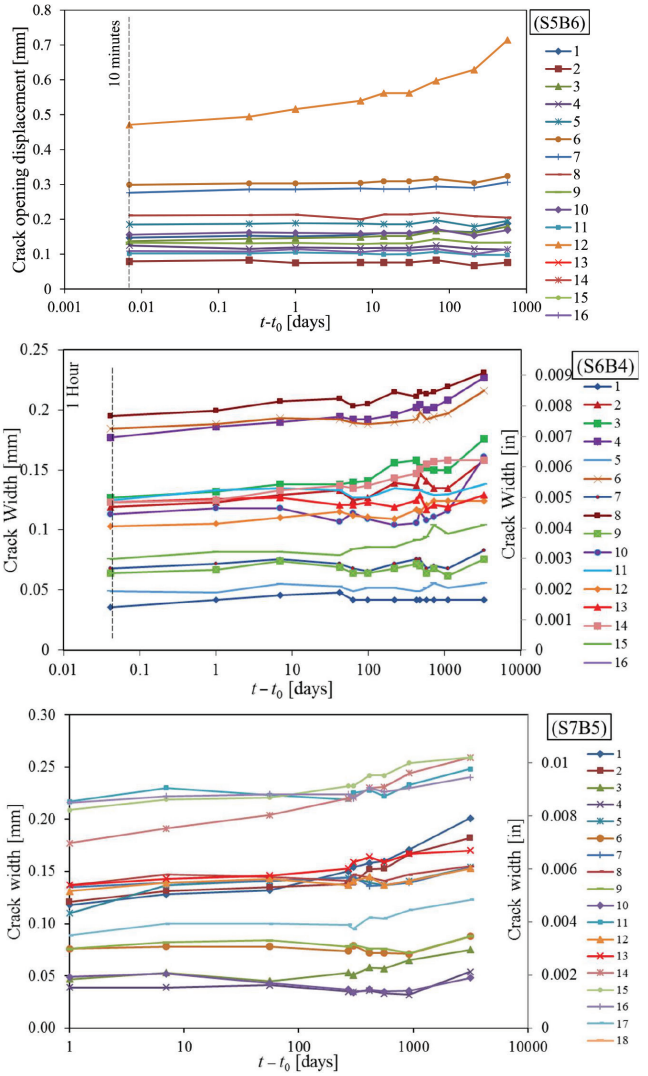

Fig. 10—Development of crack width in: (a) Specimen S5B6, 600 days under sustained loading (λ = 0.86); (b) Specimen S6B4, 3300 days under sustained loading (λ = 0.92); and (c) Specimen S7B5, 3150 days under sustained loading (λ = 0.93).

becomes zero at the crack tip. In the case of flexural cracks, the crack's maximum opening is typically at the bottom fiber of the beam. However, for an inclined shear crack that opens in tension, the crack width is primarily controlled by the reinforcement at the bottom, and the widest part of the crack is typically found at approximately midheight of the beam. To determine the maximum opening of each crack, a measuring grid comprising 241 lines and 96 points was necessary to cover the cracked surface of the beam (refer to Fig. 4).

For the major cracks at the surface of the beams, a hand-operated manual LVDT device was used to measure crack width. This method was employed for the beams of batches 5 to 7. As depicted in Fig. 10(a) to (c), the development of crack width, measured at the widest part of each crack, is tracked over time. Minor cracks of less than 100 mm (3.94 in.) in length were not considered in this measurement. The evolution of crack width over time can be categorized into three cases:

Table 4—Development of average crack width in time and evolution of midspan deflection

Specimen	$f_{c,cube,\ 28days}$, MPa	$t - t_0^*$, days	$\Delta(t)/\Delta(t_0) - 1$	$w(t)/w(t_0)$		
				Mean – 1	SD	COV
S5B4	44.1	784	0.346	0.135	0.228	0.201
S5B6	44.1	600	0.291	0.098	0.172	0.157
S6B4	81.2	3300	0.398	0.263	0.157	0.124
S6B6	81.2	1113	0.461	0.161	0.226	0.195
S7B5	80.7	3150	0.298	0.277	0.197	0.155

*In this table, t_0 is the time at which the first measurement of crack width has been conducted, which is usually 10 minutes to 1 hour after load application.

Note: 1 MPa = 145 psi.

1. Significant increase: Some cracks, such as No. 12 in S5B6, exhibit a substantial increase in crack width over time (52%). This is typically observed in the longest shear cracks on the beam's surface.

2. Dormant or slight widening: Most cracks remain dormant or display only minor widening over time.

3. Reduction followed by widening: A few cracks, such as No. 10 in S6B4, initially experience a reduction in crack width for a period, but eventually, the crack width tends to increase again. This behavior is attributed to stress redistribution within the beam, with the reduced stresses around these cracks causing the initial decrease in crack width. However, due to the creep effect, the cracks reopen over time.

The ratio of the crack width at time t to the crack width at time t_0 was calculated as $w(t)/w(t_0)$ for each crack. The development of the average crack width, standard deviation (SD), and COV are presented in Table 4. The mean increase in crack width over time ranges from 9.8% (S5B6) to 27.7% (S7B5), with the highest individual increase in crack width reaching 53%. It is important to note that the duration of sustained loading varied among the different beams under study.

Table 4 provides the ratio of midspan deflection Δ at time t to the midspan deflection Δ at time t_0. When comparing the rates of crack width development and the development of midspan deflection in the tested beams, it becomes evident that the increase in crack width over time is significantly smaller than the evolution of midspan deflection over time. However, there is also an observable correlation between these two parameters.

Shear resistance after sustained loading

To evaluate the impact of sustained loading on the shear resistance of reinforced concrete beams, those concrete beams that did not fail during the sustained loading period (12 beams) were subsequently subjected to ultimate capacity tests. Compressive strength tests were conducted concurrently with the beam tests to gain an understanding of the development of concrete strength over time. By replacing f_{ck} in Eq. (1) with the time-dependent parameter of $f_{ck}(t)$, a time-dependent shear capacity, $V_{u,calc}(t)$, can be calculated. The ratio of $V_{u,calc}(t)$ to the short-term shear capacity at t_0, $V_{u,mean}(t_0)$, can be explained as

$$V_{u,calc}(t)/V_{u,mean}(t_0) = [f_{ck}(t)/f_{ck}(t_0)]^{1/3} \quad (5)$$

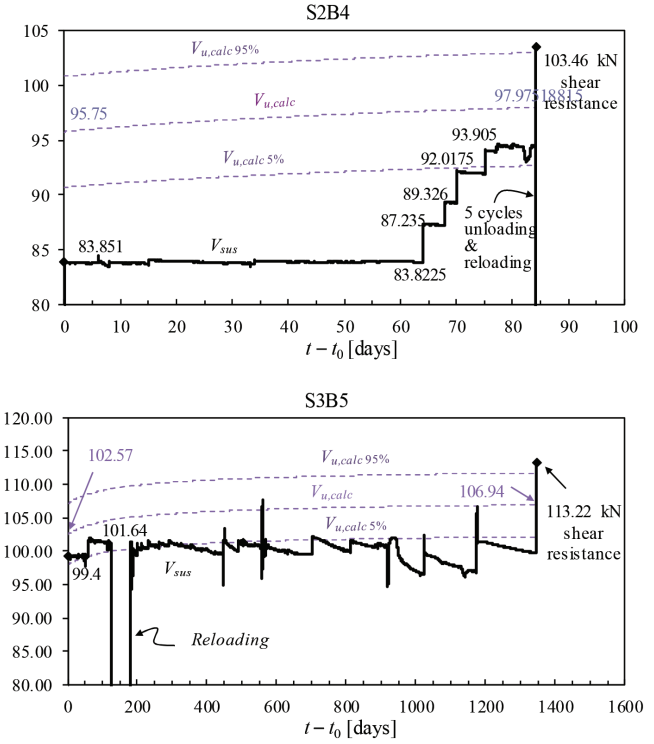

Fig. 11—Shear resistances of beams S2B4 (λ = 0.88) and S3B5 (λ = 0.97) determined at end of sustained loading period and compared with calculated shear resistance $V_{u,calc}$ *based on actual concrete strength at time* t. *Five cycles of unloading and reloading were conducted for beam S2B4 at* V_{sus} *= 93.9 kN before testing ultimate shear resistance.*

The results are presented in Fig. 11 and 12. These graphs compare the shear resistance after sustained loading with the calculated shear resistance of the beam, $V_{u,calc}$, concerning the short-term shear resistance, $V_{u,mean}$, and the concrete strength at the given time. Several observations can be made:

1. The sustained load on Specimen S2B4 after 64 days was increased step-by-step to exceed the characteristic value (lower confidence limit $V_{u,calc\ 5\%}$). After any load increment, the load was kept constant for 4 to 6 days (refer to Fig. 11). At the age of 84 days, the specimen was subjected to five cycles of unloading and reloading. Nevertheless, no failure occurred. Subsequently, the load was increased to failure. The shear resistance was found to be 103.46 kN (23,260 lb), which corresponds with the 95% (upper) fractile of the

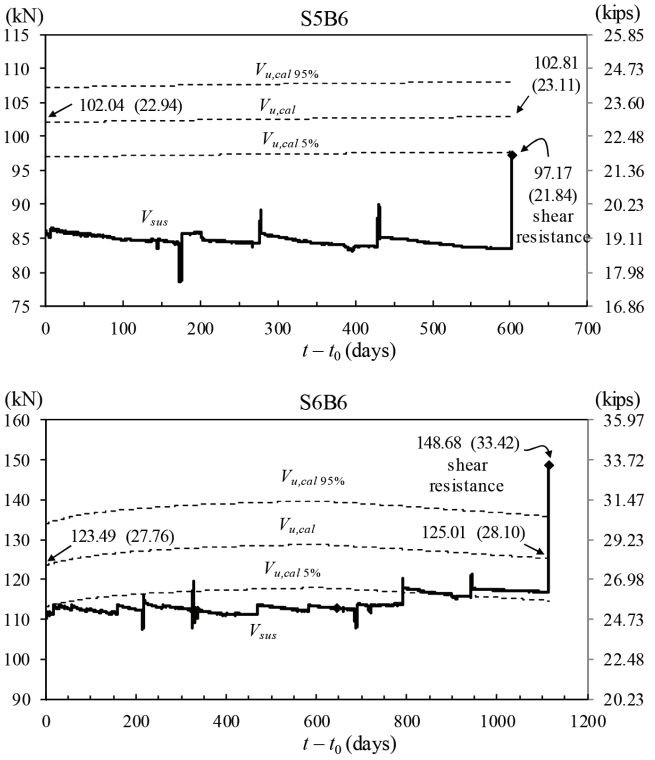

Fig. 12—Shear resistances of beams S5B6 (λ = 0.86) and S6B6 (λ = 0.92) determined at end of sustained loading period and compared with calculated shear resistance $V_{u,calc}$ *based on actual concrete strength at time* t.

calculated shear resistance, $V_{u,calc\ 95\%}$, according to the real-time concrete strength.

2. In the case of Specimen S3B5, it was temporarily unloaded after 127 days due to maintenance requirements. It was reloaded 60 days later, reaching a load of 101.6 kN (~22,841 lb), as shown in Fig. 11. The sustained loading continued for a total of 1344 days before the load was further increased to failure. The shear resistance was determined to be 113.22 kN (25,450 lb), which corresponds to the 95% fractile of the calculated (theoretical) shear resistance, $V_{u,calc\ 95\%}$, based on the real-time concrete strength.

3. For Specimen S5B6, the sustained load, which was applied for 600 days, was increased until failure, as depicted in Fig. 12. The shear resistance was determined to be 97.17 kN (21,840 lb), equivalent to the 5% characteristic value of the calculated shear resistance, $V_{u,calc\ 5\%}$. This represents the lowest value of $V_{u,exp}/V_{u,calc}$ in the batches. The progression of the width of the dominant inclined crack is illustrated in Fig. 10(a).

4. Specimen S6B6, subjected to sustained loading for 1113 days, had its load increased to the ultimate capacity and eventually the failure, as seen in Fig. 12. The shear resistance was determined to be 148.68 kN (33,425 lb), which exceeds the 95% characteristic value of the calculated shear resistance.

5. In the case of specimen S6B4, the sustained loading was halted after 3300 days. Remarkably, the beam did not exhibit any failure or crack propagation during this extended duration of sustained loading. Following the cessation of sustained loading, the load was increased until the beam reached its failure point to assess its ultimate capacity. The shear resistance, $V_{u,exp}$, was determined to be 141.99 kN (31,920 lb) after nearly a decade of high-intensity loading.

6. Sustained loading of Specimen S7B5 concluded after 3150 days, and the beam exhibited no signs of failure or crack propagation during this extended period. Following the cessation of sustained loading, the beam was loaded until it failed, allowing for the determination of its ultimate capacity. The shear resistance, $V_{u,exp}$, was measured to be 135.61 kN (30,486 lb) after nearly 8.5 years of loading.

A summary of the shear resistances after long-term loading is presented in Table 5. As demonstrated by Sarkhosh[9] and Sarkhosh et al.,[10] the ultimate shear resistance of the beams at the end of the test, $V_{u,exp}$, which had experienced long-duration high-intensity sustained loads with $\lambda > 0.86$, generally exceeded the theoretically calculated shear resistance, $V_{u,calc}$, at time t. This observation can be attributed to the conservative nature of the design expressions used for the time-dependent capacity of concrete beams, as opposed to the actual gain in concrete strength due to cement hydration.

Table 5 indicates that the actual ultimate shear capacity, $V_{u,exp}$, of the beams in this experiment, on average, exceeded the calculated value, $V_{u,calc}$, by approximately 8%. This phenomenon is likely attributed to stress relaxation in the concrete, particularly around the crack tip. In other words, the static shear resistance of the beams was scarcely affected by the load history of the specimens.

Analysis of results

The apparent contradiction between the dominant role of sustained loading effects on concrete strength in compression and tension and their absence in the shear resistance of reinforced concrete members, which is directly related to concrete strength, can be explained by considering the nature of shear cracks. As depicted in Fig. 1, the primary governing inclined shear crack, just before failure, is curved. This crack initiates as a bending crack and progresses toward the point of load application. Figure 13(a) provides a schematic representation of the behavior of such a curved crack. In this figure, the point O represents the crack tip. As the crack opens, the sections on both sides of the crack face rotate around the point O. This means that at point Y, near the crack tip, the crack opens without any shear displacement of the crack faces. However, at the more distant point X, the crack cannot open without some shear displacement of the crack faces, leading to shear-friction forces within the crack. This phenomenon is a result of aggregate interlock, as discussed by Walraven[11] and illustrated in Fig. 13(b).

In this enlarged view of the immediate surroundings of point X, the crack typically propagates around the stronger and stiffer aggregate particles, which act as barriers against the shear displacement of the crack faces. Between the aggregate particles and the cement matrix, contact areas are generated due to opposing shear displacements δ_t of the crack faces, which resist the further opening of the shear crack. This situation is more favorable than the opening of a crack in pure bending, as shown in Fig. 2. Therefore, the crack propagation at the crack tip is impeded by the aggregate interlock stresses in the lower part of the crack. Additionally,

Table 5—Shear resistance at end of long-term sustained loading

Specimen	t_0, days	t, days	$f_{c,cube}(t_0)$, MPa	$f_{c,cube}(t)$, MPa	$V_{u,mean}(t_0)$, kN	$V_{u,calc}(t)$, kN	$V_{u,exp}$, kN	$V_{u,exp}/V_{u,calc}(t)$
S2B4	72	156	39.5	41.6	95.75	97.82	103.46	1.06
S2B5	72	156	39.5	41.6	95.75	97.82	102.51	1.05
S2B6	72	156	39.5	41.6	95.75	97.82	105.03	1.07
S3B5	87	1431	51.8	57.7	102.57	106.94	113.22	1.06
S3B6	87	214	51.8	54.5	102.57	104.65	100.85	0.96
S4B4	71	345	51.0	55.6	98.63	102.00	116.40	1.14
S4B5	71	345	51.0	55.6	98.63	102.00	118.42	1.16
S5B4	512	1296	55.7	56.9	102.04	102.90	116.41	1.13
S5B6	696	1296	56.2	56.9	102.04	102.57	97.17	0.95
S6B4	113	3413	89.3	94.6	123.49	126.11	141.99	1.13
S6B6	113	1226	89.3	92.7	123.49	124.61	148.68	1.19
S7B5	219	3369	93.6	96.0	114.78	124.63	135.61	1.09
						Average		1.08
						SD		0.074
						COV		0.068

Note: 1 kN = 224.81 lb; 1 MPa = 145 psi.

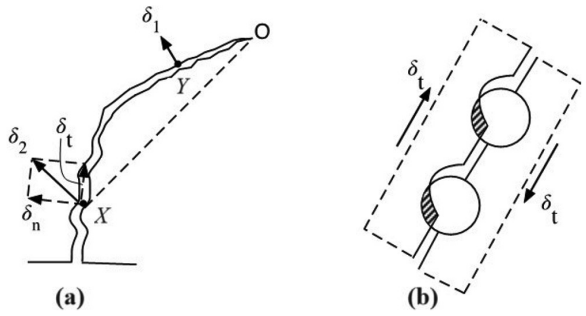

Fig. 13—(a) Curved bending-shear crack; and (b) principle of aggregate interlock at point X.

the aggregate interlock in the lower part of the crack is still in the "hardening phase," and it responds immediately by forming larger contact areas when the crack opens.

Sarkhosh[7] expanded upon an existing behavioral model initially developed by Gastebled and May[8] to account for the effects of sustained loading. This model was extended to address shear resistance under prolonged loading conditions. Additionally, Sarkhosh et al.[12] contributed to this area of research.

Furthermore, at Delft University of Technology, a novel behavioral model for the shear resistance of members lacking shear reinforcement was developed. This model places particular emphasis on the behavior of curved or bilinear bending-shear cracks, as exemplified in Fig. 13. This work can be further explored in the research conducted by Yang.[13] For another recent study on shear-transfer mechanisms in shear cracks, refer to Cavagnis et al.[14]

CONCLUSIONS

Based on the results of this experimental investigation, the following conclusions are drawn:

1. In the context of sustained loading and the time to fracture of cracked plain (unreinforced) concrete in flexure or tension, the following observations were made: When the load intensity factor (λ) is below 0.7, the time to fracture under sustained loading tends to infinity. This means the structure can withstand the load without experiencing failure for an extended period when the load is relatively low. However, when the load intensity factor exceeds 0.7, failure occurs when the total strain at time t, which is the combined effect of short-term loading and creep, exceeds a critical strain value, $\varepsilon_{c,max}(t)$. These observations suggest that the response of plain concrete under sustained loading is influenced by the applied load intensity, and failure is associated with the accumulation of strains over time. In that view, a strength reduction factor of 0.6 to 0.85, as suggested by some codes, should be applicable to unreinforced concrete under tensile or flexural loading.

2. The diagonal shear cracks, typically exceeding 100 mm (3.94 in.) in length, are considered to be significant contributors to the ultimate failure of reinforced concrete beams under sustained loading. An important observation from the study is that these major shear cracks tend to cease propagation after approximately 6 months of sustained loading under consistent conditions of temperature and humidity. This behavior suggests that once these major cracks stabilize, their contribution to the structural failure process becomes limited, and the structural integrity of the beam remains relatively stable over extended periods of time under sustained loading conditions. This observation highlights the complexity of shear crack behavior in concrete elements and underscores the need for further research to fully understand and predict the stress redistribution in a cracked concrete beam.

3. Over time, a general increase in shear resistance is observed for the reinforced concrete beams that underwent sustained loading. The actual ultimate shear capacity,

$V_{u,exp}$, of the beams in this experiment, on average, exceeds the calculated value, $V_{u,calc}$, by approximately 8%. This can be attributed to the continuous development of concrete strength due to cement hydration as well as stress redistribution and relaxation in the concrete, particularly around the crack tip. In that view, the sustained loading effect, which is known to apply to concrete subjected to axial compression or axial tension, does not apply to the shear resistance of structural concrete members without shear reinforcement, although this is a direct function of the concrete strength.

4. This comprehensive experimental program involving numerous full-scale reinforced concrete beams subjected to shear tests, including some enduring nearly a decade of long-term sustained loading, provides compelling evidence that the actual shear capacity of aging concrete structures can exceed expectations. Even when certain structural elements exhibit visible shear cracks, the research demonstrates the potential for these structures to maintain substantial shear resistance. This finding challenges conventional assumptions about the performance and durability of aged concrete infrastructure, suggesting that under certain conditions, these structures can maintain their structural integrity and safety, even with the presence of shear cracks. The residual shear resistance of old concrete bridges may be determined based on the actual concrete strength obtained from drilled cylinders. A reduction in the effect of sustained loading is not required.

5. Despite the extended research program and the substantial time of observation, some aspects could, of course, be further discussed. For instance, the test beams were, in the classical way, designed so that no failure in bending needed to be expected. It might be wondered whether the behavior under sustained loading would have been similar if the longitudinal reinforcement had been reduced to the minimum cross-sectional area possible to avoid bending failure in the tests. In recent years, better behavioral models for the determination of the shear capacity have been developed, even including the contribution by aggregate interlock in the cracks and the effect of the bending moment in the region where the shear resistance is determined. Those models form part of new modernized codes like the new version of EN 1992-1-1. Such models could also contribute to an improved understanding of the effect of aggregate interlock in neutralizing the effect of sustained loading.

AUTHOR BIOS

Reza Sarkhosh *is a Senior Civil and Structural Engineer at Shell. He received his BS from Isfahan University of Technology, Isfahan, Iran, in 2004; his MSc in earthquake engineering from Amirkabir University of Technology, Tehran, Iran, in 2006; and his PhD degree from Delft University of Technology, Delft, the Netherlands, in 2014. He is also a chartered civil engineer (CEng).*

Joost Walraven *is a Professor Emeritus at Delft University of Technology, where he received his MSc and PhD in civil engineering. His research interests include the development of advanced models for the behavior of concrete structures and new types of concrete.*

NOTATION

A_{sl}	=	cross-sectional area of tensile reinforcement
b_w	=	smallest web width
$C_{Rd,c}$	=	design factor to shear resistance according to Eurocode 2
d	=	effective depth of cross section
$f_{c,cube}$	=	compressive strength of cubes
f_{ck}	=	characteristic cylindrical compressive strength
$f_{ck}(t)$	=	characteristic compressive strength at age t
f_{ct}	=	concrete tensile strength
f_{ctk}	=	characteristic axial tensile strength of concrete
f_r	=	modulus of rupture in ACI 318-19
k	=	size factor
$V_{Rd,c}$	=	design shear resistance
V_{sus}	=	sustained shear load
V_u	=	shear resistance at ultimate state
$V_{u,calc}$	=	calculated shear resistance
$V_{u,calc\ 5\%}$	=	lower confidence limit (5% fractile) or characteristic value of calculated shear resistance
$V_{u,calc\ 95\%}$	=	upper confidence limit (95% fractile) of calculated shear resistance
$V_{u,exp}$	=	experimental shear resistance
$V_{u,mean}$	=	mean value of experimental shear resistance of beams in same batch
ρ_l	=	longitudinal reinforcement ratio

REFERENCES

1. EN 1992-1-1:2023, "Eurocode 2 - Design of Concrete Structures - Part 1-1: General Rules and Rules for Buildings, Bridges and Civil Engineering Structures," European Committee for Standardization, Brussels, Belgium, 2023, 402 pp.

2. ACI Committee 318, "Building Code Requirements for Structural Concrete (ACI 318-19) and Commentary (ACI 318R-19) (Reapproved 2022)," American Concrete Institute, Farmington Hills, MI, 2019, 624 pp.

3. Walraven, J. C., "The Influence of Effective Depth on the Shear Strength of Lightweight Concrete Beams without Shear Reinforcement," Stevin Laboratory Report No. 5-78-4, Delft University of Technology, Delft, the Netherlands, 1978, 36 pp.

4. *fib*, "*fib* Model Code for Concrete Structures (2020)," International Federation for Structural Concrete, Lausanne, Switzerland, 2024, 780 pp.

5. Tasevski, D.; Fernández Ruiz, M.; and Muttoni, A., "Influence of Load Duration on Shear Strength of Reinforced Concrete Members," *ACI Structural Journal*, V. 117, No. 2, Mar. 2020, pp. 157-170.

6. Zhou, F., and Hillerborg, A., "Time-Dependent Fracture of Concrete: Testing and Modelling," *Fracture Mechanics of Concrete Structures: Proceedings of the First International Conference (FraMCoS1)*, Z. P. Bažant, ed., Breckenridge, CO, June 1992, pp. 906-911.

7. Sarkhosh, R., "Shear Resistance of Reinforced Concrete Beams without Shear Reinforcement under Sustained Loading," PhD thesis, Delft University of Technology, Delft, the Netherlands, 2014, 285 pp.

8. Gastebled, O. J., and May, I. M., "Fracture Mechanics Model Applied to Shear Failure of Reinforced Concrete Beams without Stirrups," *ACI Structural Journal*, V. 98, No. 2, Mar.-Apr. 2001, pp. 184-190.

9. Sarkhosh, R.; Walraven, J.C.; den Uijl, J.A.; and Braam, C.R., "Shear Capacity of Concrete Beams under Sustained Loading," *Proceedings of the 9th fib International PhD Symposium in Civil Engineering*, H. S. Müller, M. Haist, and F. Acosta, eds., Karlsruhe, Germany, July 2012, pp. 29-34.

10. Sarkhosh, R.; Walraven, J. C.; and den Uijl, J. A., "Shear-Critical Reinforced Concrete Beams under Sustained Loading - Part I: Experiments," *HERON*, V. 60, No. 3, 2015, pp. 181-206.

11. Walraven, J. C., "Aggregate Interlock: A Theoretical and Experimental Analysis," PhD thesis, Delft University of Technology, Delft, the Netherlands, 1980, 210 pp.

12. Sarkhosh, R.; Walraven, J. C.; and den Uijl, J. A., "Shear-Critical Reinforced Concrete Beams under Sustained Loading - Part II: Numerical Study," *HERON*, V. 60, No. 3, 2015, pp. 207-234.

13. Yang, Y., "Shear Behaviour of Reinforced Concrete Members without Shear Reinforcement: A New Look at an Old Problem," PhD thesis, Delft University of Technology, Delft, the Netherlands, 2014, 370 pp.

14. Cavagnis, F.; Fernández Ruiz, M.; and Muttoni, A., "An Analysis of the Shear-Transfer Actions in Reinforced Concrete Members without Transverse Reinforcement Based on Refined Experimental Measurements," *Structural Concrete*, V. 19, No. 1, Feb. 2018, pp. 49-64. doi: 10.1002/suco.201700145